J Nanopart Res (2024) 26:60
https://doi.org/10.1007/s11051-024-05972-x

RESEARCH PAPER

Comprehensive characterizations of organoclay types based on their integration to poly (butylene terephthalate) nanocomposites

Yildiz Bas · Ali Sinan Dike

Received: 20 September 2023 / Accepted: 14 March 2024 / Published online: 18 March 2024

Abstract Polybutylene terephthalate (PBT) nanocomposites loaded with two different types of organoclays are fabricated using the melt mixing technique in a twin-screw extruder. Quaternary ammonium salts with dimethyl, benzyl, hydrogenated tallow, and dimethyl, dehydrogenated tailed modified organoclays are blended with PBT matrix at the compositions of 1%, 3%, 5%, and 10% weight ratios. Test samples are shaped using a lab-scale injection molding device. Mechanical, thermo-mechanical, thermal stability, melt flow, structural, and morphological behaviors of the nanocomposite samples are investigated by performing tensile, impact, and shore hardness tests, dynamic mechanical analysis (DMA), thermo-gravimetric analysis (TGA), melt flow rate measurements, X-ray diffraction analysis (XRD), and scanning electron microscopy (SEM) methods, respectively. According to the findings, NC 130 clay gave better results than NC 140 in terms of tensile, hardness, and melt flow behaviors, whereas NC 140 showed higher performances as impact resistance, thermo-mechanical, and density, since the reduction in density and weight lowering are highly required for mainly transportation sector, and thermal properties were considered.

Keywords Poly (butylene terephthalate) · Nanocomposites · Organoclay · Polymer composites · Biomedicine · Antidiabetic · Antimicrobial · Antioxidant · Thermal properties

Y. Bas · A. S. Dike (✉)
Department of Nanotechnology and Engineering Sciences, Adana Alparslan Turkes Science and Technology University, 01250 Adana, Türkiye
e-mail: asdike@atu.edu.tr

A. S. Dike
Materials Engineering Department, Adana Alparslan Turkes Science and Technology University, 01250 Adana, Türkiye

Introduction

Composite materials are simply described as a mixture containing reinforcement additives embedded in a matrix. Matrix is the continuous phase and reinforcing material is the discontinuous phase in the composite system. The combination of these two phases results in improved properties concerning the property of each constituent. A nanocomposite is a multiphase solid substance in which one of the phases has a diameter of fewer than 100 nm (nm) or structures with nanoscale repeat intervals between the various phases. In the case of dispersing small amounts of nanofillers into polymer matrices, mechanical behavior, gas, and solvent barrier properties, thermal degradation, and chemical resistance can be improved while avoiding traditional micro-filler drawbacks such as embrittlement, loss of transparency, and lightness [1–4].

Clay minerals are hydrous aluminum phyllosilicates, also known as layered silicates, that include diverse cations such as iron, magnesium, and alkali metals. These clay minerals are quite abundant and

may be found in a variety of environments, including sedimentary rocks [5–7]. Clays are made up of tetrahedral and octahedral sheets. The ratio of these two sheets in the structure is used to categorize the structure. In the stacking morphology of clay particles, for example, a 2:1 clay structure shows that one octahedral sheet is sandwiched between two tetrahedral sheets. While clay minerals can have both 1:1 and 2:1 structures, the 2:1 structure, often known as a smectite structure, is more frequent in clay products. Bonding between the tetrahedral and octahedral sheets in the development of a 2:1 structure requires that the tetrahedral sheet be corrugated or twisted, resulting in a ditrigonal distortion of the hexagonal array, followed by flattening of the octahedral sheet. This reduces the total distortion forces of the crystallite, resulting in a layered flat form. Small molecules can easily intercalate between these layers since they are weakly packed together with a regular van der Waals gap [8, 9]. As a result, the phyllosilicates most typically utilized in the creation of nanocomposite materials, such as montmorillonite, hectorite, and saponite, belong to the structural family of 2:1 layered silicates. The basic raw material for nanoclay products is montmorillonite (smectite clay). The surface features of smectite clay minerals may be modified due to their plate-like structure. Following treatment with organic modifiers, the beginning basal spacing between these plates is about 15; after treatment with organic modifiers, the basal spacings are approximately 32–36 Angstrom. Increased basal spacing results in more homogenous dispersion inside polymer structures [10, 11].

Poly (1, 4-butylene terephthalate) (PBT) is a synthetic semi-crystalline thermoplastic that belongs to the polyester group of resins and has properties comparable to other thermoplastic polyesters. It is a high-performance material with an excellent balance of mechanical and electrical characteristics, as well as strong dimensional stability, heat resistance, and processing benefits. PBT is readily moldable and thermoformable [12, 13]. However, it is well known that thermal, oxidative, and hydrolytic degradation can occur at the processing temperature (250–280 °C). PBT is gradually damaged by thermo- and photo-oxidative processes that occur over its lifespan, depending on the temperature and outdoor usage. Furthermore, its flammability and severe dripping during combustion restrict its applicability; this is why the thermal breakdown of polyesters such as poly (ethylene terephthalate) (PET) and PBT has remained a focus of research [14–16].

In recent years, polymer–clay nanocomposites have been studied by many researchers. In one of these studies, Santiago et al. performed the production of organoclay-filled poly (sodium acrylate) composites. They investigated the enhancement in thermal stability and swelling behavior after the addition of organoclay [17]. Singh and Ghosh examined the torsional, structural, and tensile behavior of organoclay-reinforced acrylonitrile butadiene styrene (ABS) terpolymer composites using melt mixing. They found that the rigidity and modulus of elasticity of ABS were improved by the addition of organoclay [18]. Dike and Yilmazer performed several research studies related to polystyrene nanocomposites loaded with different types of organoclays. They implied that aliphatic and aromatic elastomers can be integrated into polymer/clay systems as compatibilizers to promote intercalation and exfoliation structures for clay layers into a polystyrene matrix. They proved that elastomeric and aliphatic compatibilizers act as dispersion enhancers for nanoclay layers into the polymeric phase [19, 20]. Guven et al. used calcium organoclay as an additive in a polymer emulsion of styrene-co-butyl acrylate copolymer [21]. Additionally, superabsorbent applications of organoclay containing various polymer composites were also studied in the literature [22–24]. Akar et al. prepared polyamide-6 (PA-6) composites filled with two types of organoclays in a recently published study. Their findings suggested that organo-modified clay inclusions caused an increase in the thermal, structural, and mechanical performance of PA-6 [25]. Ge et al. studied the influence of silane coupling agents on the tribological performance of organoclay-filled nitrile butadiene rubber-based composites [26]. Kraus et al. performed the thermal, mechanical, and morphological characterizations of organoclay-filled low-density polyethylene (LDPE)–based composites to predict the surface properties of composites [27]. Similarly, Seyidoglu and Yilmazer reported that compatibilizer addition increased the mechanical properties of organoclay-loaded linear LDPE composites [28]. Investigations dealing with LDPE-based composites filled with organoclay were also performed by Majeed et al. They evaluated the barrier performance of LDPE/clay nanocomposite films after the inclusion of compatibilizer containing anhydride-grafted polyethylene and they obtained extension in interlayer spacing between clay layers through the PBT phase [29]. Dogan and Tayfun examined the use of

organoclay in the melt spinning process of poly (lactic acid) (PLA) fiber in terms of dyeability. They postulated that organoclay inclusions led to an increase in tensile strength and dyeability, whereas a reduction in percent crystallinity of PLA fiber [30]. Keyfoglu and Yilmazer proposed the influence of chain extension–branching agent modification of nanoclay in addition to tunning process parameters to PET-based nanocomposites. They revealed that composites filled with maleic anhydride–modified organoclay at the loading level of 3% exhibited the best performance based on structural and mechanical behaviors [31]. Liborio et al. applied a treatment method for organoclay and they fabricated organoclay-filled polypropylene-based composites by using extrusion [32]. Suhas et al. integrated sulfonic acid–treated clay for the fabrication of composite membranes which were used for pervaporation dehydration of isopropanol [33]. Additionally, numerous research works were reported to investigate the flame retardancy of nanoclay-containing polymers thanks to the establishment of synergistic interactions between flame retardant reagents and organoclay. According to these studies, it can be deduced that organoclays can be effectively used for the development of thermally stable and fire-resistive polymeric composites in the presence of phosphorus and boron-based flame retardants [34–44].

PBT polymer was also studied in research works dealing with the polymer/organoclay composite system. For instance, there have been several published works found in the literature that are related to organoclay-filled polymer nanocomposite systems for a variety of industrial applications. Xiao et al. prepared clay/PBT nanocomposite through a direct melt intercalation method using thermally stable organically modified montmorillonite as filler. They also found a remarkable improvement in melting temperature and rate of crystallization of the resulting clay/PBT nanocomposites. Twin-screw extrusion was also used for melt intercalation of clay/PBT nanocomposites [45]. Another example is the study of Chang et al. in which they prepared clay/PBT nanocomposites through in situ interlayer polymerization and found that the thermal and mechanical properties of PBT can be enhanced by the dispersion of a very small amount of organoclay exceedingly [46]. Quispe and coworkers conducted a study with composites based on post-industrial waste or primarily recycled PBT and 5 wt.% of organically modified montmorillonite clays using a twin-screw extruder and melt blending technique. It is a good example of how improvements can be achieved on the physical properties of recycled PBT with a small content of organically modified montmorillonite to add value to primarily recycled engineering thermoplastics [47]. In a study by Acierno et al. performed in 2004, the effect of organoclay inclusion on the structure and properties of a PBT-based nanocomposite system was investigated. In terms of mechanical properties, the silicate nanoscale dispersion significantly increased the stiffness and reduced the ductility compared to PBT. They also experienced weight loss by organoclay inclusions during hybrid compounding. They concluded that the absorbed volatile fraction by the PBT matrix causes compositional changes and a decrease in the thermal stability of composites [48]. Saeed et al. in 2015 prepared kaolin clay/PBT composite films by solution casting technique. They confirmed the dispersion of kaolin into the PBT matrix by SEM analysis. They concluded that the size of spherulites of PBT was decreased by the incorporation of clay into PBT due to the nucleation effect of kaolin clay. The mechanical properties of clay/PBT composites were significantly enhanced concerning neat PBT and the thermal stability of PBT was improved up to 10 °C by the addition of kaolin into the polymer matrix [49]. Li et al. conducted a comprehensive assessment of polymer–clay nanocomposite (PCN) systems. They tried to show how the organic modifiers affect the polymer crystallinity and elastic modulus of PCN systems. Nanoclay exhibited an intercalated and partially exfoliated structure, whereas organoclay formed intercalation in the PBT phase due to the strong interactions between ammonium cation and silicate layers of organoclay [50]. Katti et al. conducted a comprehensive study of PBT/clay and PA6/clay nanocomposite systems based on molecular dynamics and experimental techniques. Although the same amount of modified clay was used in the preparation steps of composites, they observed dramatic changes in crystallinity and improvement in mechanical properties. According to their findings, polymers with higher crystallinity required significantly higher attractive and repulsive interaction energies between polymers and their modifiers to reach a similar change in crystallinity compared to other polymers having lower crystallinity [51]. In another research reported by Nirukhe et al. three different intercalating agents were used to prepare different organically modified montmorillonite (MMT). They fabricated PBT/clay nanocomposites by melt mixing

with clay compositions ranging from 1 to 5 wt%. They observed that composites involving intercalating agents yield high thermal stability stems from the pyridinium cations compared to neat clay. They concluded that mechanical and thermal properties strongly depended on the nanocomposite structure and clay content. It was found that the addition of a small amount of organoclay (up to 3 wt%) was enough to level up the mechanical properties of PBT. They also showed that the inclusion of organoclay affects the crystallinity of the polymer since the clay acts as a nucleating agent according to DSC analysis [52]. Soudmand et al. investigated the toughness of PBT-based nanocomposites filled with nanoclay based on mechanical characterizations and subsequent microstructural observations. In their study, clay and nano-precipitated calcium carbonate were selected as nano-reinforcing phases. They showed that the fracture morphology of compact tension samples showed a low extent of plastic deformation for neat PBT. According to their results, relative to PBT, the stress intensity factor increased up to 57% and 45% with the addition of clay. They implied that nanocomposites displayed a crack initiation zone of fibrillated morphology [53].

Nanoclay-filled polymeric materials have some limitations in terms of their performance in various applications due to poor interface adhesion between clay layers and the polymer phase. This study's novelty originates in the evaluation of the influence of two distinct types of organoclay additives on structural, mechanical, thermal, thermo-mechanical, physical, and morphological characteristics of PBT-based nanocomposites thanks to contributions of comprehensive performance characterization based on two kinds of nanoclay modified with quaternary ammonium salts with dimethyl, benzyl, hydrogenated tallow and dimethyl, dehydrogenated tallow. Investigations were conducted after the fabrication step of nanocomposites using melt extrusion process followed by an injection molding technique. The basic difference of this research from those described in previously published works is the experimental evaluation of property enhancement of PBT nanocomposites after being compounded with organoclays based on the dispersion promoter effect of ammonium salts through nanoclay interlayers into PBT matrix. Organoclay samples and prepared composites were subjected to X-ray spectroscopy and SEM study to visualize the structural and morphological properties. In addition to mechanical performances such as tensile, hardness, and impact tests, thermal (TGA), thermo-mechanical (DMA), physical behaviors including density, and melt flow measurements were reported for basic understanding and comparison of the influences of two grades of organoclays.

Table 1 The chemical compositions of organoclays

Composition (%)	NC 130	NC 140
Al_2O_3	11.37	6.67
SiO_2	49.80	44.3
Na_2O	0.16	0.70
Fe_2O_3	0.59	0.41
K_2O	0.31	0.30
CaO	0.33	0.47
MgO	2.43	1.41
TiO_2	0.04	0.04
d value (Å)	34.66	38.62

Materials

Organoclay powders used in this study were supplied from Eczacıbaşı Esan, İstanbul, Türkiye. Two kinds of nanoclay grades were used with the commercial names of esanNANO 2–130 (NC 130) and esanNANO 1–140 (NC 140) which were coated by different quaternary ammonium salts containing dimethyl, benzyl, hydrogenated tallow, and dimethyl, dehydrogenated tallow, respectively. The chemical composition obtained from X-ray fluorescence analysis and basalt spacing parameter (*d* value) estimated by X-ray diffractometry analysis of organoclay grades is listed in Table 1. NC 130 clay has

Table 2 Compositions of prepared composites

Sample codes	PBT content (wt%)	NC 130 content (wt%)	NC 140 content (wt%)
PBT	100	0	0
PBT/1% NC 130	99	1	0
PBT/3% NC 130	97	3	0
PBT/5% NC 130	95	5	0
PBT/10% NC 130	90	10	0
PBT/1% NC 140	99	0	1
PBT/3% NC 140	97	0	3
PBT/5% NC 140	95	0	5
PBT/10% NC 140	90	0	10

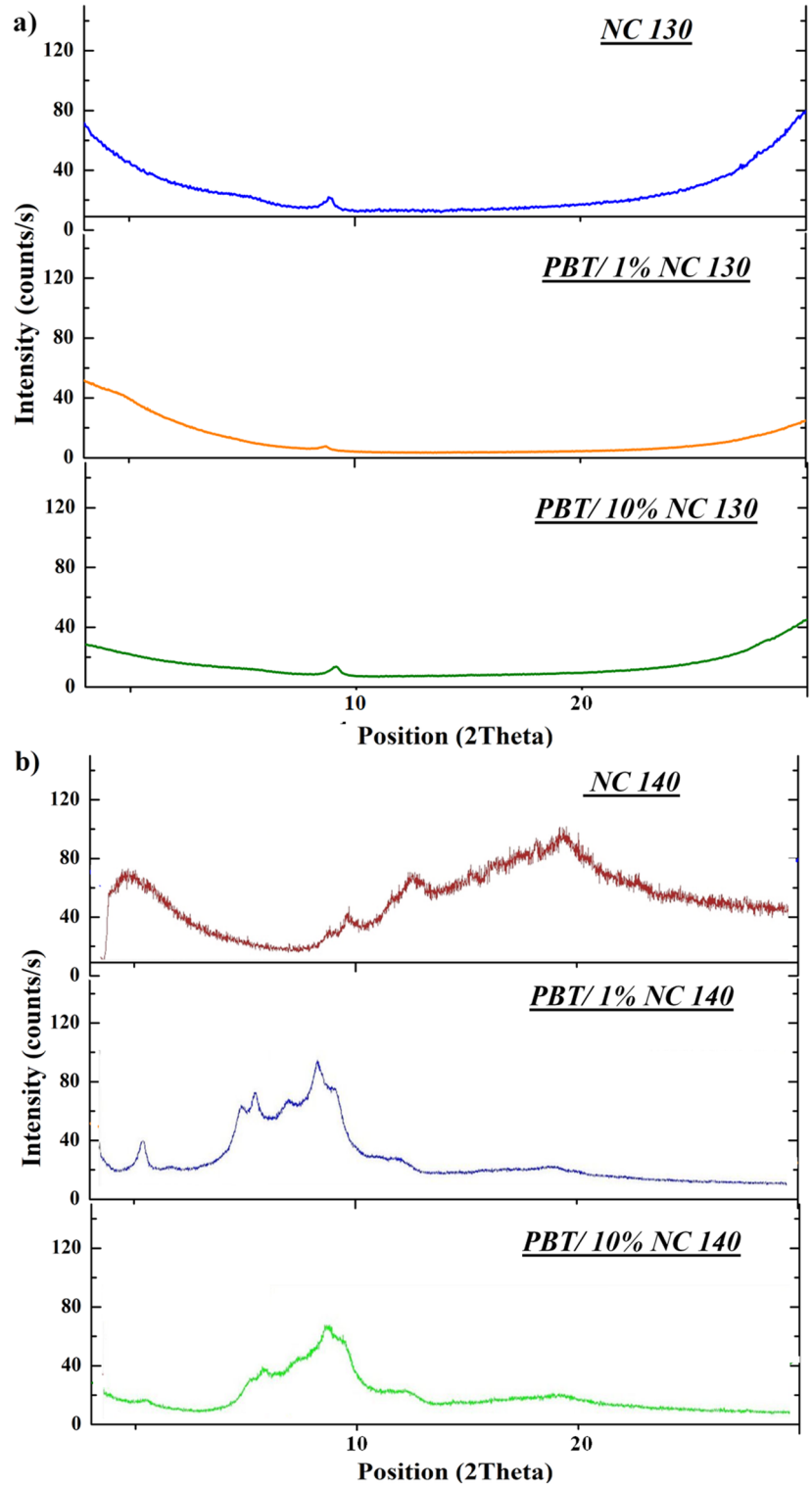

Fig. 1 XRD curves of nanoclays, PBT, and composites

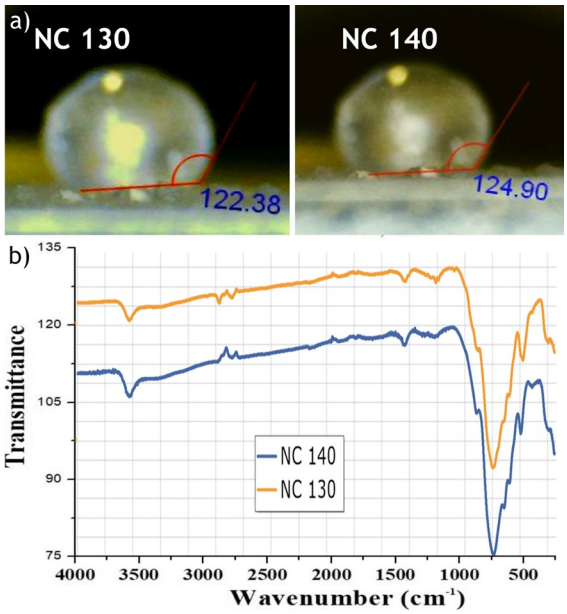

Fig. 2 Contact angle images (**a**) and FTIR spectra of nanoclays (**b**)

a yellowish color and NC 140 is pure white-colored. The commercial PBT thermoplastic polymer was purchased from Sasa Polyester A.Ş. (Adana, Türkiye) with the trade name Advanite SB88. This PBT grade has a viscosity of 0.90 dL/g and a melt flow rate of 33 g/10 min.

Experimental methods

Preparation of composites

PBT chips and organoclay powders were pre-dried at 100 °C for 2 h using an oven (FN 055, Nuve A.Ş., Ankara, Türkiye). PBT chips and organoclay powders were compounded by a twin-screw 15 cc Xplore micro-extruder (MC 15 HT, Xplore Instruments). The processing temperature of 240 °C, mixing time of 5 min, and mixing speed of 100 rpm were applied during the compounding process. Neat PBT was also mixed using the same processing parameters and named PBT. Loading amounts of NC 130 and NC 140 into the PBT matrix were 1, 3, 5, and 10 by weight % and the contents of composites are listed in Table 2. After the extrusion process, composites were obtained in chip form, and dog bone–shaped test samples with the dimensions of $80 \times 7.5 \times 2.5$ mm^3 were prepared using a micro-injection molding machine (Micro-injector, Daca Instruments) at a barrel temperature and mold temperature of 245 °C and 80 °C, respectively.

Characterization methods

The structural investigations of organoclays, PBT, and organoclay-filled PBT nanocomposites were carried out by XRD analysis using X'Pert PRO, PAN analytical with Ni-filtered CuKα radiation ($\lambda = 0.154$ nm) at 40 mA and 45 kV. XRD device utilized. FTIR analysis in attenuated total reflectance mode was carried out by BrukerVERTEX70 IR-spectrometer at a resolution of 2 cm^{-1} with 32 scans in the range of 600 and 3800 cm^{-1} wavenumbers. Veho VMS-004D PC-controlled optical microscope was utilized for performing contact angle measurements. The digital pictures were captured at 400 magnification, and the contact angle data was determined using Veho VMS-004D software. Tensile tests were performed using a universal tensile testing device (Lloyd LR 30 K, West Sussex, UK). Tests were done with dog bone test samples

Table 3 Mechanical test results of PBT and composites

Sample codes	Tensile strength (MPa)	Youngs' modulus (GPa)	Elongation at break (%)	Impact strength (kJ/m^2)	Hardness (Shore D)
PBT	34.0 ± 0.8	0.64 ± 0.3	9.1 ± 0.4	9.5 ± 0.6	75.0 ± 0.1
PBT/1% NC 130	42.8 ± 0.4	0.72 ± 0.1	11.6 ± 0.8	16.4 ± 0.7	72.6 ± 0.2
PBT/3% NC 130	43.5 ± 0.3	0.73 ± 0.1	12.7 ± 0.7	14.9 ± 0.4	74.3 ± 0.2
PBT/5% NC 130	42.7 ± 0.3	0.75 ± 0.2	10.8 ± 0.8	11.5 ± 0.4	75.5 ± 0.1
PBT/10% NC 130	41.4 ± 0.2	0.73 ± 0.1	10.3 ± 0.5	9.6 ± 0.3	77.1 ± 0.2
PBT/1% NC 140	40.7 ± 0.4	0.63 ± 0.2	11.2 ± 0.6	18.8 ± 0.6	69.8 ± 0.2
PBT/3% NC 140	42.1 ± 0.2	0.65 ± 0.1	12.4 ± 0.4	15.2 ± 0.5	71.4 ± 0.1
PBT/5% NC 140	41.6 ± 0.3	0.66 ± 0.2	12.2 ± 0.3	13.5 ± 0.3	73.0 ± 0.2
PBT/10% NC 140	40.8 ± 0.2	0.59 ± 0.2	12.0 ± 0.3	10.5 ± 0.4	75.2 ± 0.1

using parameters of 5 kN load cell and 10 mm/min as crosshead speed according to ASTM D-638 standard. Coesfeld impact tester device (Coesfeld GmbH, Dortmund, Germany) was utilized to investigate the impact energy values of PBT and its composite samples using a 4 J pendulum. Shore hardness tests were performed by the Zwick Roell R5LB041 hardness analyzer. Shore D hardness values of test samples were recorded according to ISO 7619–1 standard procedure. TGA analyses were done by applying a heating rate of 10 °C/min using Perkin Elmer Diamond TG/DTA thermal test equipment (Massachusetts, USA). Analysis was carried out under the nitrogen atmosphere with a flow rate of 50 mL/min in the heating range of 25–650 °C. DMA investigations were done using dual cantilever bending mode in a 25–200 °C temperature range and 10 °C/min constant heating rate by utilizing Hitachi HT (Tokyo, Japan), DMA7100 analyzer under the nitrogen atmosphere. Melt flow measurements of unfilled PBT and composite samples were estimated using Coesfeld Meltfixer LT (Dortmund, Germany). The standard load of 2.16 kg was used at 240 °C during MFR measurements. Density measurements were applied to PBT and composite samples using a Mettler Toledo (Ohio, USA) Easy D30 digital density meter in which average results of recorded values of at least three samples were reported. Before SEM analysis was conducted, cyro-fractured surfaces of samples were coated with a conductive layer of gold. SEM images of composites were taken with magnifications varied from 1000 to 10,000 by FEI (Orean, USA) Quanta 400F FESEM scanning electron microscope device. For TEM investigation, sections of 70 nm in thickness of composite samples were cryogenically cut with a diamond polymer knife at a temperature of − 100 °C for composite samples. Prepared samples were trimmed parallel to the molding direction and analyzed by an FEI Transmission Electron Microscope at an acceleration rate of 80 kV.

Results and discussion

Structural analysis of clay samples and composites

XRD curves NC 130 clay, PBT polymer, and PBT/NC 130–coded composite samples are given in Fig. 1a. The characteristic peaks of both organoclays can be seen at nearly 2θ = 8° from their curves in Fig. 1. This peak started to disappear for NC 130 and NC 140 as the adding amount increased. It can be observed from XRD curves of composites with 10% content of both organoclays; this characteristic peak was completely lost. The absence of this peak in the XRD curve of a composite indicates that clay layers intercalated into a polymer matrix [54, 55].

XRD curves NC 140 clay, PBT polymer, and PBT/NC 140 named composite samples are shown in Fig. 1b. The Bragg peaks of composite samples seen at around the 2θ = 15–20° range are related to the distance between clay layer and named d-spacing [56, 57]. The magnitude of this peak was found to be increased for PBT/1% NC 140 and PBT/10% NC 140 composites. According to these findings, NC 140 clay exhibited more significant improvement in terms of intercalation and dispersion of organoclay plates into the PBT phase.

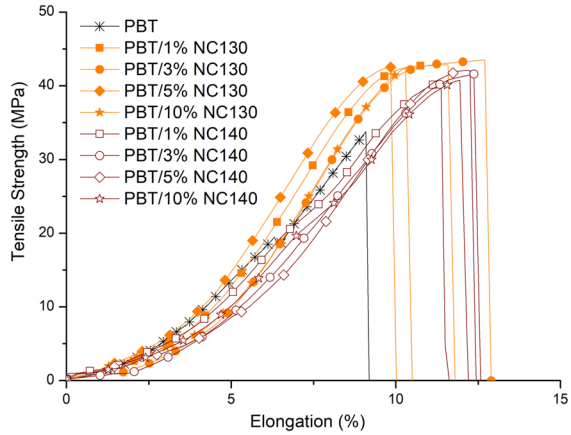

Fig. 3 Stress versus strain curves of PBT and composites

Table 4 Thermal analysis results of PBT and composites

Sample codes	$T_{5\%}$ (°C)	$T_{10\%}$ (°C)	T_{max} (°C)	char (%)
PBT	359	370	441	1.2
PBT/1% NC 130	360	372	447	3.3
PBT/3% NC 130	358	369	442	4.0
PBT/5% NC 130	357	370	439	5.7
PBT/10% NC 130	361	371	444	8.9
PBT/1% NC 140	368	375	504	3.1
PBT/3% NC 140	367	374	488	3.7
PBT/5% NC 140	366	375	459	5.6
PBT/10% NC 140	368	377	447	9.5

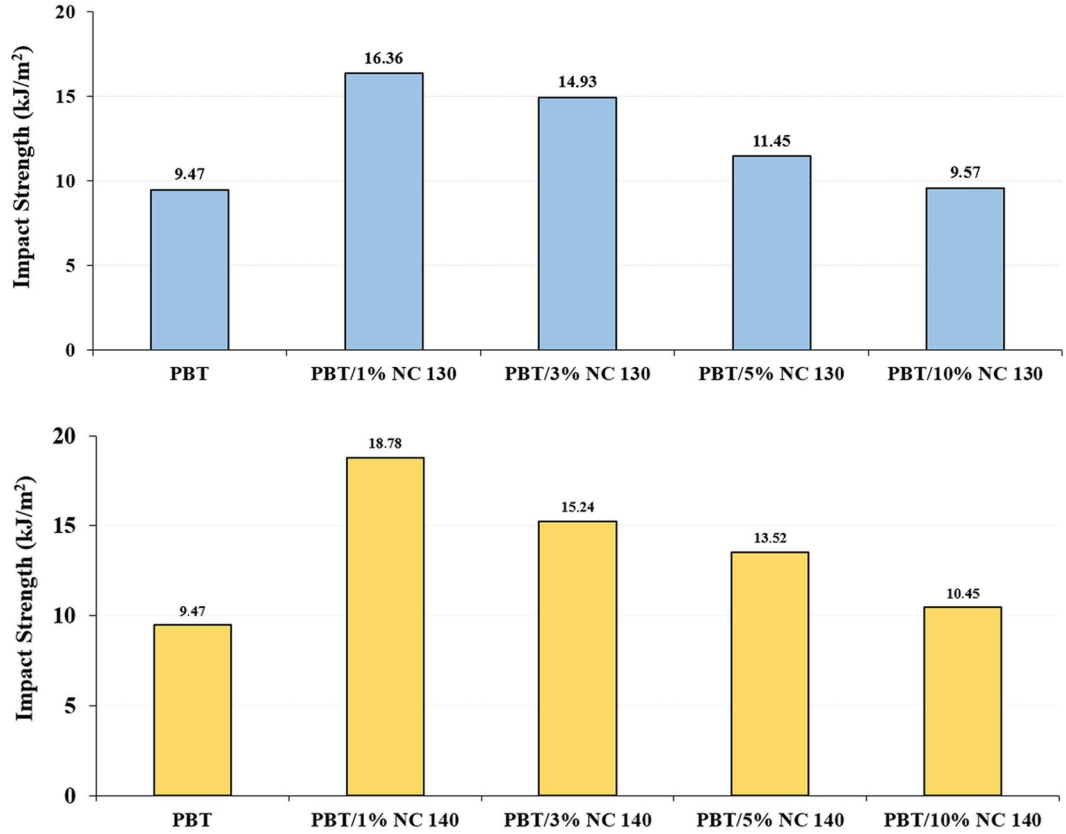

Fig. 4 Impact test results of composites

As visualized with contact angle images in Fig. 2a, contact angle values of NC 130 and NC 140 clays were obtained as 122.4° and 124.9°. This result indicated that the presence of the benzyl group in hydrogenated tallow on the NC 140 surface reduced surface hydrophobicity concerning NC 130 clay due to the absence of the benzyl functionality in dimethyl tallow on the NC 130 surface. The reason for obtaining high contact values stems from the quaternary ammonium salts on nanoclay surface.

The FTIR spectra of clay samples are displayed in Fig. 2b. The absorption peak at around 2900 cm^{-1} indicated -CH vibrations due to the presence of methyl groups on nanoclay surfaces. IR spectra of clay samples exhibited hydroxyl group peaks with high intensities centered at 750 and 3600 cm^{-1}, indicating O–H stretching vibrations. The characteristic peak stemming from the N–H stretching vibrations around 1600 cm^{-1} on the spectra of both NC 130 and NC 140 may be caused by the nitrogen-containing hydrocarbon groups in quaternary ammonium functionality. These findings validated the surface coatings on nanoclay samples.

Tensile behaviors of composites

Mechanical test data of PBT and its composites including tensile parameters, impact strength values, and hardness parameters are listed in Table 3. The tensile strength of PBT was found to be 34 MPa. NC 130 clay additions gave distinct improvements to the strength value of PBT. The greatest result was obtained for 3% NC 130–filled composite among all of the prepared samples. The amount of increase in tensile strength for this sample was estimated approximately as a 28% improvement concerning that of PBT. Composites reinforced with NC 130 clays yielded higher strength values compared to NC 140–containing composites. This finding indicates that NC 130 showed a better reinforcing ability to

PBT matrix than NC 140 clays which may be due to the establishment of an enhanced interaction between clay layers and the PBT phase in the presence of pendant benzyl group on the ammonium salt tallow of NC 130. Tensile strength increased by the concentration of both organoclays up to the adding amount of 3%. After that point, tensile strength reduced dramatically and the lowest strength values were obtained for the PBT/10% NC 140 sample among composites.

The strength versus strain curves of PBT and relevant composites are given in Fig. 3. The transcendence of NC 130–containing composites over NC 140–containing ones according to tensile behaviors can be observed visually from their characteristic strength versus strain curves in Fig. 3. As the elongation at break parameters was evaluated, it can be said that all of the composites showed higher elongation results than that of neat PBT. In contrast to tensile strength findings, NC 140 additions led to an increase in elongation values. NC 130 and NC 140 inclusions displayed different trends in Youngs' modulus results according to Table 4. NC 130 clay led to a distinct increase in modulus values. On the other hand, only slight improvements were obtained for composites involving NC 140. Moreover, PBT/10% NC 140 yielded a lowering for Youngs' modulus of PBT. Similar findings were observed in the case of Youngs' modulus results of polymer composites filled with nanofillers [58–60].

Hardness measurements of composites

According to shore D hardness results listed in Table 3, organoclay additions caused a decrease at lower filling ratios, initially. The hardness of composites improved as the contents of clays increased and the maximum hardness values were reached for composites involving a 10% amount of NC 130 and NC 140. Enhancement of hardness with the addition of plate-like fillers was an expected behavior thanks to the layered structure of nanoclay [61–64]. However, intercalation of NC 130 and NC 140 resulted in the reduction of the hardness of composites at low amounts of additives due to a high level of dispersion degree can be achieved. Similar

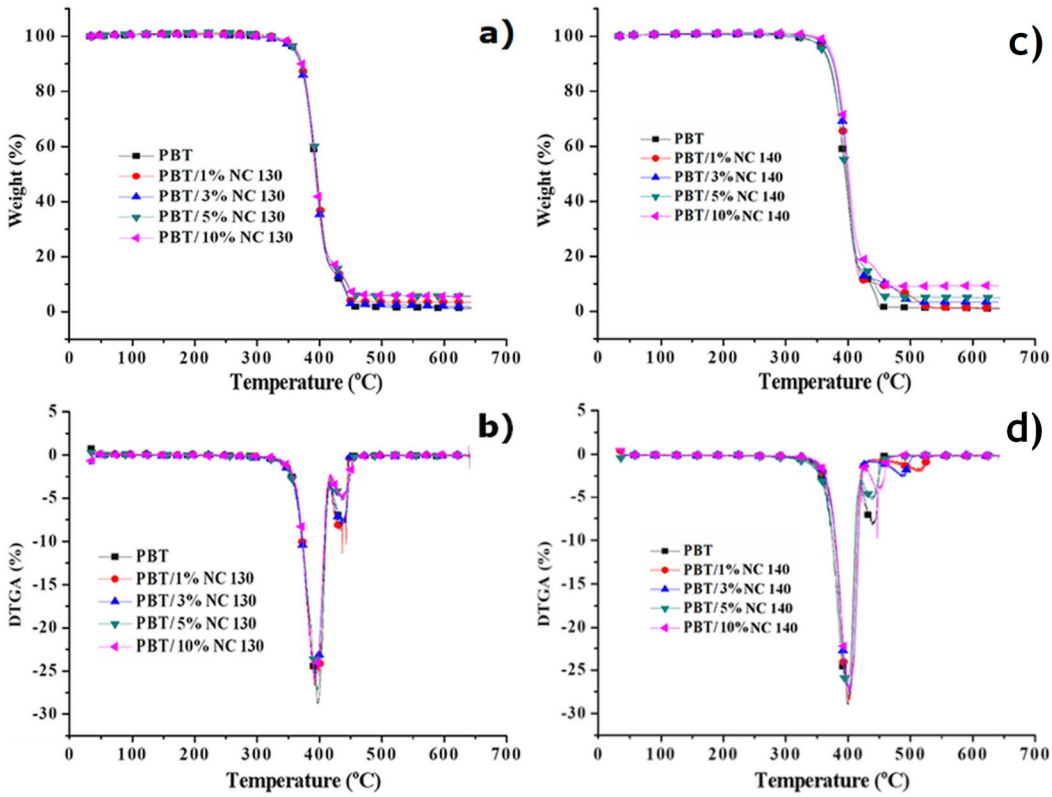

Fig. 5 TGA (**a**, **c**) and DTGA (**b**, **d**) curves of PBT/NC 130 and PBT/NC 140 nanocomposites

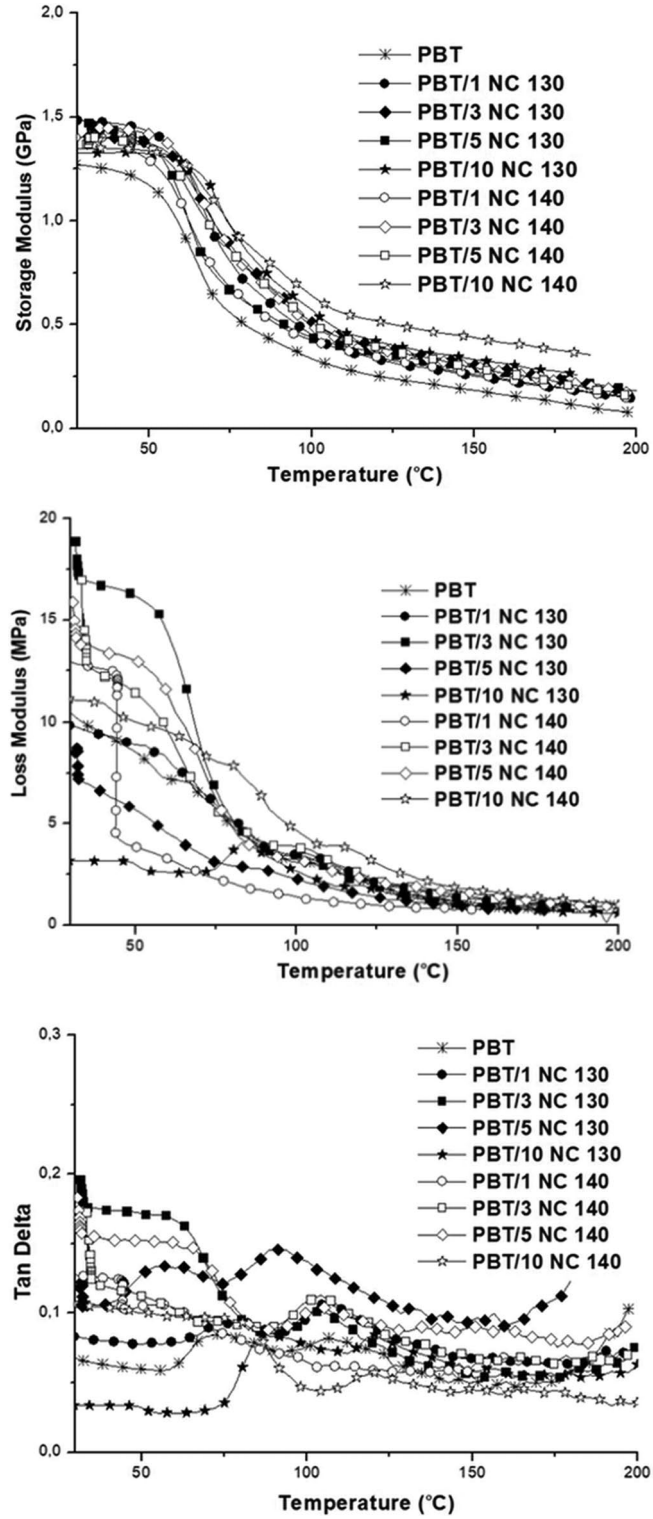

Fig. 6 DMA curves of PBT and composites

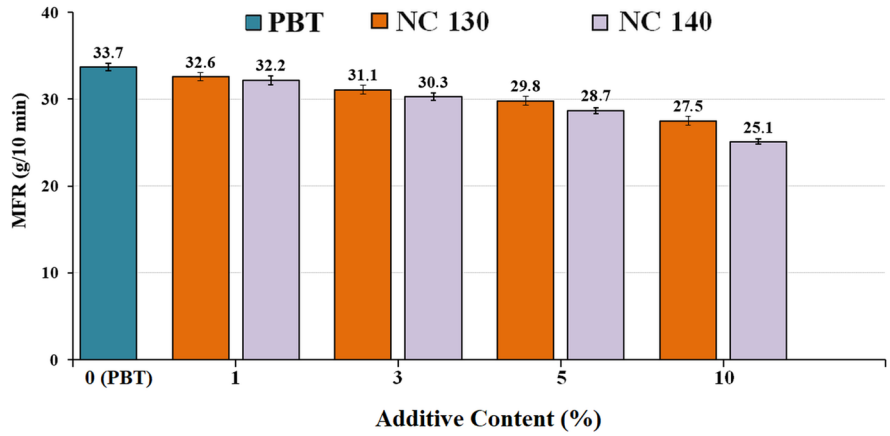

Fig. 7 MFR test results and PBT and composites

to tensile test results, NC 130 displayed higher shore hardness values compared to NC 140.

Impact resistance of composites

Figure 4 demonstrates the changes in impact strength values according to organoclay inclusions. It was observed from impact test results that organoclay-containing composites gave remarkably higher impact strength than neat PBT. The greatest impact performance was reached for composites filled with NC 140 clay at its lowest adding amount. The impact strength of PBT showed an almost twofold increase with the addition of 1% NC 140. Similarly, the PBT/1% NC 130 sample exhibited the greatest impact strength among NC 130–loaded composites. A sudden reduction in impact performance was found with further inclusions of organoclays. As a diverse trend from tensile and hardness findings, NC 140 clay yielded higher performance in terms of impact strength. This result can be explained as dimethyl, dehydrogenated ammonium modification of clay resulting in better impact resistance to crack propagation during deformation [65–67] compared to dimethyl, benzyl, hydrogenated tallow integrated NC 130 clay.

Thermal analysis of composites

TGA—DTGA curves of NC 130–containing nanocomposites versus temperature are represented in Fig. 5a and b, respectively. TGA—DTGA curves of NC 140–filled nanocomposites versus temperature are displayed in Fig. 5c and d, respectively. Thermal analysis data are shared in Table 4.

According to thermal analysis data displayed in Table 4, NC 130 additions caused no obvious changes to $T_{5\%}$ and $T_{10\%}$ parameters of PBT since nearly identical values were obtained. This observation was correlated by TGA and DTGA curves in Fig. 5. On the other hand, composites containing NC 140 led to a remarkable increase in thermal analysis values. Improvement in the thermal stability of PBT after the incorporation with NC 140 clay was visually observed in TGA and DTGA curves of composites. The presence of higher d-spacing between layers of NC 140 clay compared to NC 130 might be the reason for these findings due to the positive effect of intercalation of clay layers on the formation of a thermal barrier. For this reason, PBT/NC 140 composite samples gave higher performance than NC 130 in terms of thermal resistance. Based on the char ratios of samples, composites yielded higher residue content compared to neat PBT, as expected. NC 130 and NC 140 clays gave nearly identical char amounts at the end of the analysis.

Table 5 Density and MFR test results of PBT and composites

Sample codes	Density (g/cm^3)	MFR (g/10 min)
PBT	1.315 ± 0.2	33.7 ± 0.2
PBT/1% NC 130	1.309 ± 0.2	32.6 ± 0.1
PBT/3% NC 130	1.314 ± 0.1	31.1 ± 0.2
PBT/5% NC 130	1.328 ± 0.3	29.8±0.2
PBT/10% NC 130	1.341 ± 0.2	27.5 ± 0.3
PBT/1% NC 140	1.2970.1	32.2 ± 0.1
PBT/3% NC 140	1.308 ± 0.2	30.3 ± 0.2
PBT/5% NC 140	1.319 ± 0.1	28.7 ± 0.2
PBT/10% NC 140	1.330 ± 0.2	25.1 ± 0.1

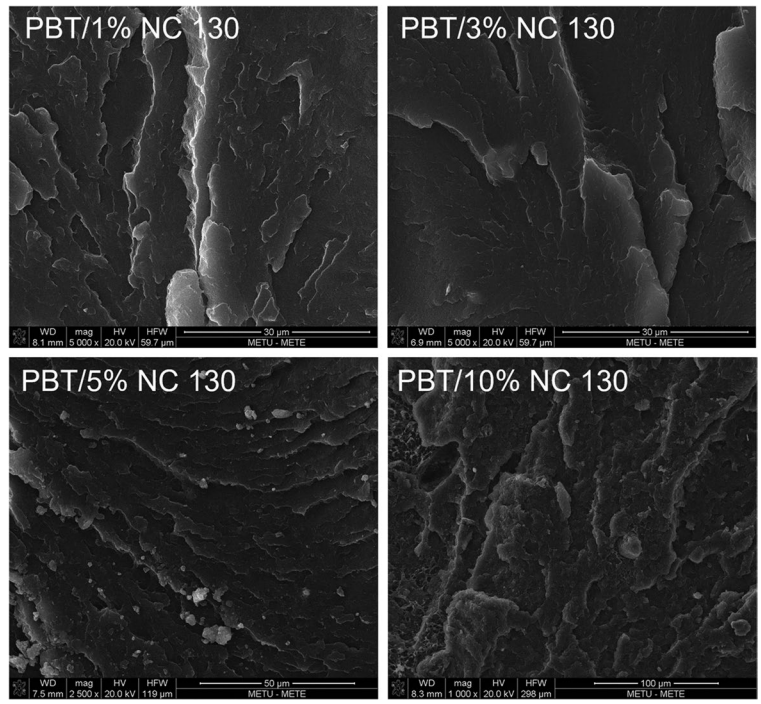

Fig. 8 SEM micro-images of PBT/NC 130 composites

Thermo-mechanical properties of composites

Thermo-mechanical parameters including storage modulus, loss modulus, and tan delta curves of PBT and its composite samples which were derived from DMA data are illustrated in Fig. 6.

The storage modulus of neat PBT extended up to higher levels with the inclusions of organoclays regardless of clay grades. Although both clay types gave nearly identical storage modulus curves, NC 140–filled composites exhibited slightly higher modulus values compared to PBT/NC 130 composites. Composite samples with 10% loading displayed the highest storage modulus levels at elevated temperatures.

According to loss modulus curves shared in Fig. 6, organoclay inclusions led to an increase in the loss modulus of neat PBT. Adding amounts of NC 130 and NC 140 showed a negative effect on the loss modulus of composites. It can be said that loss modulus values reduced as the contents of organoclays increased.

Tan delta curves of samples revealed that the peak value of PBT shifted to higher temperatures with the addition of clays. The peak temperature of the tan delta curve corresponds to the specific glass transition temperature of the polymer (T_g). Inclusions of NC 130 and NC 140 caused to increase in the T_g value of PBT.

MFR parameters of composites

MFR parameter is related to viscosity and rheology of polymeric material. MFR values of PBT and composites are indicated in bar chart format in Fig. 7 and listed as numerical data in Table 5.

MFR of neat PBT lowered with clay inclusions. Reduction of MFR carried on as additive content increased. It can be deduced that the change in MFR values obtained in a narrow range of 10% decreases for composite samples containing low amounts of NC 130 and NC 140. However, a 10% loading of clays resulted in a dramatic drop down for MFR of PBT as a 20–25% reduction. NC 140–filled composite displayed the lowest MFR value among prepared samples. As a comparison based on clay types, NC 130–loaded PBT composites gave slightly higher MFR values than that of NC 140 clay.

Density measurements of composites

The density data of neat PBT and its composites are shown in Table 5. The density of PBT was measured as 1.315 g/cm^3. Low amounts of clay inclusions gave a reduction in the density of PBT. Relatively higher density values were obtained for highly filled PBT/NC 130 and PBT/NC 140

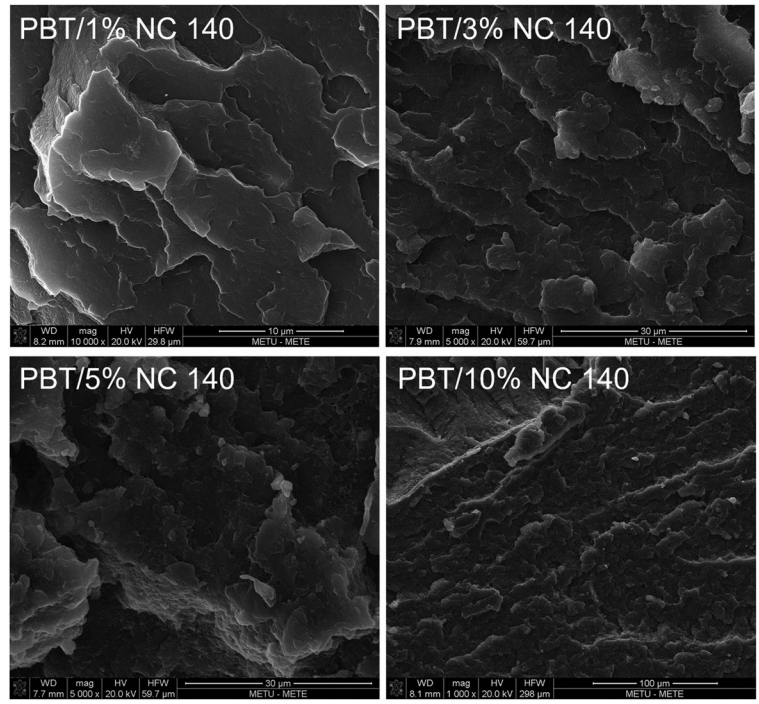

Fig. 9 SEM micro-images of PBT/NC 140 composites

composite samples. Composites involving NC 140 exhibited lower density compared to NC 130–containing composites. The lowest density value was obtained for the PBT/1% NC 140 sample in which a 1.8% decrease was measured concerning the density of PBT.

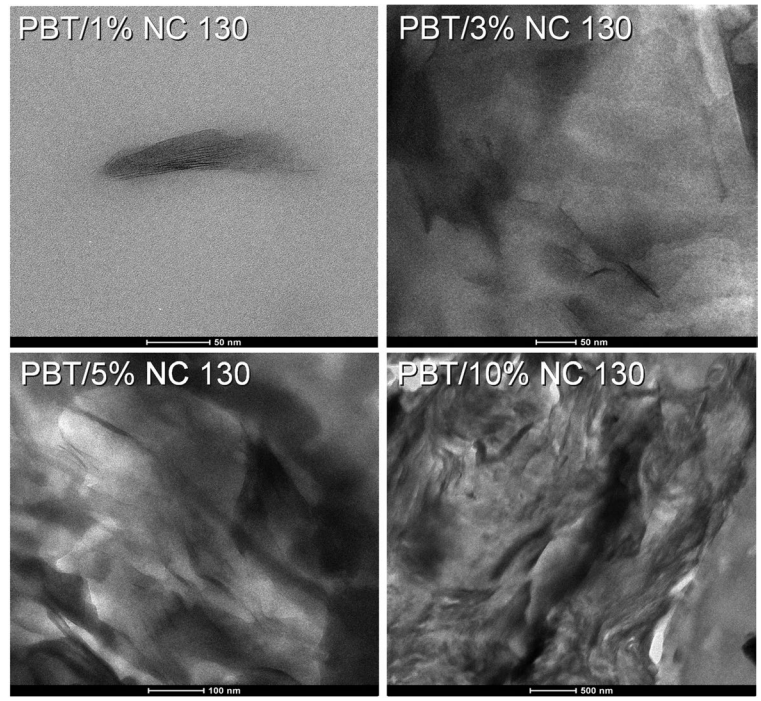

Fig. 10 TEM images of PBT/NC 130 composites

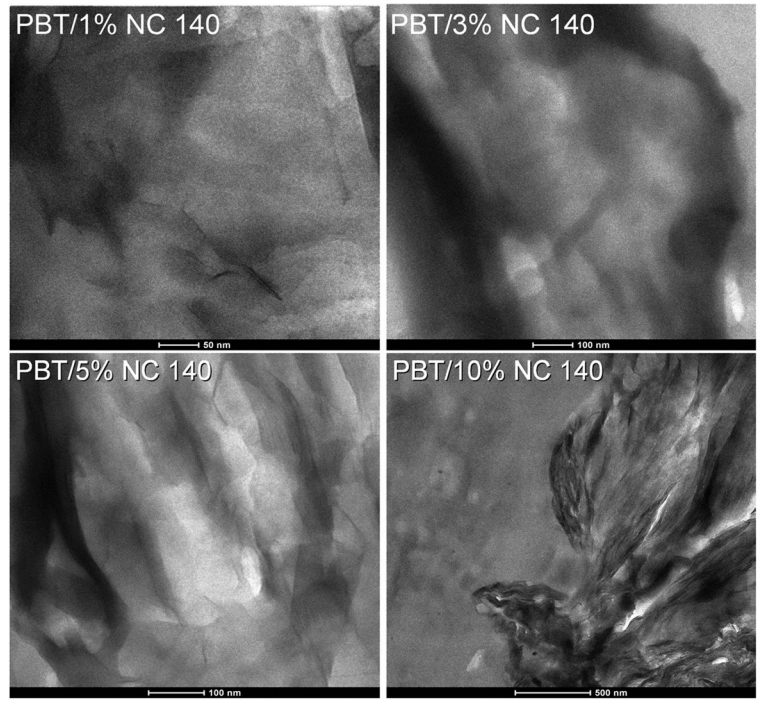

Fig. 11 TEM images of PBT/NC 140 composites

Morphological characterization of composites

SEM micro-images of composites involving NC 130 and NC 140 organoclays are represented in Fig. 8 and Fig. 9, respectively. NC 130 clay displayed uniform dispersion into the PBT phase for its low adding amounts according to SEM micro-images of PBT/1% NC 130 and PBT/3% NC 130. The formation of agglomerated clay regions was observed as the additive content increased. The poor dispersion was obtained from an SEM micro-image of the 10% NC 130–loaded composite sample in Fig. 8.

SEM micro-images of PBT/NC 140 samples in Fig. 9 exhibited similar observations in which NC 140 clay particles dispersed homogeneously into the PBT matrix at low filling ratios. Accordingly, clay particles started to form agglomerates as their concentrations increased. The decrease in the degree of dispersion for highly filled PBT/clay system as observed from SEM micro-images was the main reason for obtaining reductions for investigated performances of composites containing 10% of organoclays as described in previous results.

TEM images of the nanocomposites containing NC 130 and NC 140 organoclays are visualized in Fig. 10 and Fig. 11, respectively. Based on the TEM images, the dispersion of the clay particles was found to be more homogeneous in composites filled with low amounts of nanoclay grades. PBT/1% NC 130 in Fig. 10 exhibited the intercalated structure of the clay layers in the composite structure. Similarly, loading of 1% NC 140 displayed intercalation of clay layers according to Fig. 11. Further additions of both NC 130 and NC 140 resulted in the phase separation and loss of dispersion homogeneity of clay particles inside the PBT matrix.

Conclusions

In this current study, organoclay containing PBT-based nanocomposite materials was produced using an extrusion process. The effects of two grades of organoclay inclusions on the PBT matrix were examined by mechanical, thermal, physical, structural, thermo-mechanical, and morphological characterizations. Structural properties of PBT nanocomposites involving NC 130 and NC 140 organoclays were evaluated by XRD analysis. It was found that low amounts of both clay grades exhibited intercalated structures in the PBT phase.

Mechanical test results showed that both organoclay additions increased tensile and impact performance of PBT. The tensile strength of composites improved by up to 3% adding content to both organoclays. Further additions of clays caused a decrease in the strength values of composites. The greatest strength performance was obtained for the PBT/3% NC 130 sample. NC 130 clay displayed higher tensile strength values compared to NC 140 grade. Similar to tensile strength results, Youngs' modulus of PBT improved by the addition of organoclay powders. PBT/NC 130 composite samples gave higher Youngs' modulus values than NC 140–incorporated composites at their identical loading amounts. Elongation at break parameter of PBT was found to be enhanced after the inclusions of both clay types. Shore hardness of neat PBT exhibited a decreasing trend for lower contents of clays. However, the hardness of composites improved as the filling ratio of NC 130 and NC 140 increased. As a comparison, NC 130 grade showed higher values than NC 140 in terms of shore hardness parameter. Impact test findings revealed that organoclay additions with 1% concentration resulted in a remarkable increase in the impact strength of PBT. Further inclusions caused a reduction in the impact strength of composites. The greatest impact performance was achieved for the sample of PBT/1% NC 140. Composites containing NC 140 clay displayed better impact resistance compared to NC 130–filled composites. According to the thermal analysis conducted by TGA studies, clay incorporations resulted in improvements in the thermal stability of neat PBT. PBT/NC 140 composites gave relatively higher thermal performance than that of NC 130 clay. Thermal stability and the amount of char residue of composite samples increased by the adding ratios of organoclays. With the help of DMA test results, it was obtained that storage modulus and loss modulus curves of PBT shifted to higher values after being compounded with organoclays. NC 140–containing composites displayed higher performance compared to NC 130 in terms of storage modulus and loss modulus results. Tan delta curves implied that additions of both organoclays yielded a significant increase in the glass transition temperature of PBT. As density measurements were examined, the density value of PBT was found to be decreased in the case of low loadings of NC 130 and NC 140. PBT/NC 140 composite samples exhibited lower density values than NC 130–containing composites as their identical filling amounts were compared. Melt flow test showed that the MFR parameter of PBT was reduced by the addition of clay powders. All of the composite samples gave lower MFR values compared to neat PBT. Composites filled with NC 130 clay yielded slightly higher results compared to NC 140 in terms of MFR parameters. The morphology and dispersion quality of each composite sample were claimed by SEM images. Organoclay particles exhibited uniform dispersion for composites containing low contents (1% and 3%) of clays. On the contrary, poor dispersion of clays was observed with the help of SEM micro-images of PBT/10% NC 130 and PBT/10% NC 140 samples.

Author contribution Y. Bas: analysis, experimental and data curation, and writing—original draft; A.S. Dike: supervision, investigation, formal analysis, validation, methodology, methodology, and writing—review and editing.

Data availability The data that support the findings of this study are available on request from the corresponding author.

Declarations

Ethical approval Ethical approval is not applicable for this study.

Consent to participate The authors confirm that all information they provide for this study is realistic experimental data and findings.

Conflict of interest The authors declare no competing interests.

References

1. Balazs AC, Emrick T, Russell TP (2006) Nanoparticle polymer composites: where two small worlds meet. Science 314(5802):1107–1110
2. Dubey KA, Hassan PA, Bhardwaj YK (2017) High performance polymer nanocomposites for structural applications. materials under extreme conditions. Elsevier 2017:159–194
3. Grimsdale AC, Müllen K (2005) The chemistry of organic nanomaterials. Angew Chem 44:5592–5629
4. Rao CN, Müller A, Cheetham AK (2006) The chemistry of nanomaterials: synthesis, properties and applications. John Wiley & Sons, New Jersey
5. Albdiry M, Yousif B, Ku H, Lau K (2013) A critical review on the manufacturing processes in relation to the

properties of nanoclay/ polymer composites. J Compos Mater 47(9):1093–1115
6. Floody MC, Theng BKG, Reyes P, Mora ML (2009) Natural nanoclays: applications and future trends–a Chilean perspective. Clay Miner 44(2):161–176
7. Okamoto M (2006) Polymer/layered silicate nanocomposites. Int Polym Proc 21(5):487–496
8. Gao F (2004) Clay/polymer composites: the story. Mater Today 7(11):50–55
9. Jlassi K, Chehimi MM, Thomas S (2017) Clay-polymer nanocomposites. Elsevier, Amsterdam
10. Ray SS, Okamoto M (2003) Polymer/layered silicate nanocomposites: a review from preparation to processing. Prog Polym Sci 28(11):1539–1641
11. Zanetti M, Lomakin S, Camino G (2000) Polymer-layered silicate nanocomposites. Macromol Mater Eng 279:1–9
12. Abobo IMD, Rodrigez LD, Salvador SD, Siy HC, Penaloza DP (2021) Effect of organoclay reinforcement on the mechanical and thermal properties of unsaturated polyester resin composites. Epitoanyag-J Silicate Based Compos Mater 73(2):128
13. Gallo E, Braun U, Schartel B, Russo P, Acierno D (2009) Halogen-free flame retarded poly (butylene terephthalate) (PBT) using metal oxides/PBT nanocomposites in combination with aluminium phosphinate. Polym Degrad Stab 94(8):1245–1253
14. Hong JS, Kim YK, Ahn KH, Lee SJ, Kim C (2007) Interfacial tension reduction in PBT/PE/clay nanocomposite. Rheol Acta 46:469–478. https://doi.org/10.1007/s00397-006-0123-1
15. Chisholm BJ, Moore RB, Barber G, Khouri F, Hempstead A, Larsen M, Olson E, Kelley J, Balch G, Caraher J (2002) Nanocomposites derived from sulfonated poly (butylene terephthalate). Macromolecules 35(14):5508–5516
16. Samperi F, Puglisi C, Alicata R, Montaudo G (2004) Thermal degradation of poly (butylene terephthalate) at the processing temperature. Polym Degrad Stab 83(1):11–17
17. Santiago F, Mucientes AE, Osorio M, Rivera C (2007) Preparation of composites and nanocomposites based on bentonite and poly (sodium acrylate). Effect of amount of bentonite on the swelling behaviour. Eur Polymer J 43:1–9
18. Singh P, Ghosh AK (2014) Torsional, tensile and structural properties of acrylonitrile–butadiene–styrene clay nanocomposites. Mater Des 55:137–145
19. Dike AS, Yilmazer U (2020) Improvement of organoclay dispersion into polystyrene-based nanocomposites by incorporation of SBS and maleic anhydride-grafted SBS. J Thermoplast Compos Mater 33(4):554–574
20. Dike AS, Yilmazer U (2020) Mechanical, thermal and rheological characterization of polystyrene/organoclay nanocomposites containing aliphatic elastomer modifiers. Mater Res Expr 7(1):015055
21. Guven O, Karakas F, Kaya MA, Yildirim H, Celik MS (2014) Composite films based on styrene-co-butylacrylate with colemanite and calcium bentonite mineral fillers. Mech Compos Mater 50(3):335–342
22. Alexandre M, Dubois P (2000) Polymer-layered silicate nanocomposites: preparation, properties and uses of a new class of materials. Mater Sci Eng R Rep 28(1–2):1–63
23. Li A, Wang A (2005) Synthesis and properties of clay-based superabsorbent composite. Eur Polymer J 41(7):1630–1637
24. Tao W, Xiaoqing W, Yi Y, Wenqiong H (2006) Preparation of bentonite–poly [(acrylic acid)-acrylamide] water superabsorbent by photopolymerization. Polym Int 55(12):1413–1419
25. Akar AO, Yildiz UH, Tayfun U (2021) Investigations of polyamide nano-composites containing bentonite and organo-modified clays: mechanical, thermal, structural and processing performances. Rev Adv Mater Sci 60(1):293–302
26. Ge X, Zhang Y, Deng F, Cho UR (2017) Effects of silane coupling agents on tribological properties of bentonite/nitrile butadiene rubber composites. Polym Compos 38(11):2347–2357
27. Kraus E, Nguen DA, Efimova A, Starostina I, Stoyanov O (2016) Acid− base properties of polyethylene composites with clays. J Appl Polym Sci 133(30):43629
28. Seyidoglu T, Yilmazer U (2012) Use of purified and modified bentonites in linear low-density polyethylene/organoclay/compatibilizer nanocomposites. J Appl Polym Sci 124(3):2430–2440
29. Majeed K, Hassan A, Bakar AA (2014) Influence of maleic anhydride-grafted polyethylene compatibiliser on the tensile, oxygen barrier and thermal properties of rice husk and nanoclay-filled low-density polyethylene composite films. J Plast Film Sheeting 30(2):120–140
30. Tayfun U, Dogan M (2016) Improving the dyeability of poly (lactic acid) fiber using organoclay during melt spinning. Polym Bull 73(6):1581–1593
31. Keyfoglu AE, Yilmazer U (2004) Effects of chain extension and branching on the properties of poly (ethylene-terephthalate)-organoclay nanocomposites. MRS Online Proceedings Library 856:BB3.6
32. Liborio P, Oliveira VA, Maria de Fatima VM (2015) New chemical treatment of bentonite for the preparation of polypropylene nanocomposites by melt intercalation. Appl Clay Sci 111:44–49
33. Suhas DP, Aminabhavi TM, Raghu AV (2014) para-Toluene sulfonic acid treated clay loaded sodium alginate membranes for enhanced pervaporative dehydration of isopropanol. Appl Clay Sci 101:419–429
34. Reddy KR, Reddy CV, Babu B, Ravindranadh K, Naveen S, Raghu AV (2019) Recent advances in layered clays–intercalated polymer nanohybrids: synthesis strategies, properties, and their applications. Modified Clay Zeol Nanocompos Mater 8:197–218
35. Yurddaskal M, Celik E (2018) Effect of halogen-free nanoparticles on the mechanical, structural, thermal and flame retardant properties of polymer matrix composite. Compos Struct 183:381–388
36. Dogan M, Dogan SD, Savas LA, Ozcelik G, Tayfun U (2021) Flame retardant effect of boron compounds in polymeric materials. Compos Part B: Eng 222:109088
37. Hu Y, Tang Y, Song L (2006) Poly (propylene)/clay nanocomposites and their application in flame retardancy. Polym Adv Technol 17:235–245
38. Qin H, Zhang S, Zhao C, Hu G, Yang M (2005) Flame retardant mechanism of polymer/clay nanocomposites based on polypropylene. Polymer 46(19):8386–8395
39. Tan Y, Xie J, Wang Z, Li K, He Z (2023) Effect of halloysite nanotubes (HNTs) and organic montmorillonite (OMMT) on the performance and mechanism of flame retardant-modified asphalt. J Nanopart Res 25(4):74

40. Doğan M, Erdoğan S, Bayramlı E (2013) Mechanical, thermal, and fire retardant properties of poly (ethylene terephthalate) fiber containing zinc phosphinate and organo-modified clay. J Therm Anal Calorim 112:871–876
41. Liu P, Guo J (2007) Organo-modified magnesium hydroxide nano-needle and its polystyrene nanocomposite. J Nanopart Res 9:669–673
42. Durmuş A, Woo M, Kaşgöz A, Macosko CW, Tsapatsis M (2007) Intercalated linear low density polyethylene (LLDPE)/clay nanocomposites prepared with oxidized polyethylene as a new type compatibilizer: structural, mechanical and barrier properties. Eur Polymer J 43(9):3737–3749
43. Oliveira SVD, Araújo EM, Pereira CMC, Leite AMD (2017) Nanocompósitos de polietileno/argila bentonítica com propriedades antichama. Polímeros 27:91–98
44. Nazare S, Kandola BK, Horrocks AR (2006) Flame-retardant unsaturated polyester resin incorporating nanoclays. Polym Adv Technol 17(4):294–303
45. Xiao J, Hu Y, Wang Z, Tang Y, Chen Z, Fan W (2005) Preparation and characterization of poly (butylene terephthalate) nanocomposites from thermally stable organic-modified montmorillonite. Eur Polymer J 41(5):1030–1035
46. Chang JH, An YU, Kim SJ, Im S (2003) Poly (butylene terephthalate)/organoclay nanocomposites prepared by in situ interlayer polymerization and its fiber (II). Polymer 44(19):5655–5661
47. Quispe NB, Fernandes EG, Zanata F, Bartoli JR, Souza DH, Ito EN (2015) Organoclay nanocomposites of post-industrial waste poly (butylene terephthalate) from automotive parts. Waste Manage Res 33(10):908–918
48. Acierno D, Scarfato P, Amendola E, Nocerino G, Costa G (2004) Preparation and characterization of PBT nanocomposites compounded with different montmorillonites. Polym Eng Sci 44(6):1012–1018
49. Saeed K, Khan I (2015) Characterization of clay filled poly (butylene terephthalate) nanocomposites prepared by solution blending. Polímeros 25:591–595
50. Li X, Kang T, Cho WJ, Lee JK, Ha CS (2001) Preparation and characterization of poly (butyleneterephthalate)/organoclay nanocomposites. Macromol Rapid Commun 22(16):1306–1312
51. Katti DR, Katti KS, Raviprasad M, Gu C (2012) Role of polymer interactions with clays and modifiers on nanomechanical properties and crystallinity in polymer clay nanocomposites. J Nanomater 2012(28):341056
52. Nirukhe AB, Shertukde VV (2009) Preparation and characterization of poly (butylene terephthalate) nanocomposites with various organoclays. J Appl Polym Sci 113(1):585–592
53. Soudmand BH, Shelesh-Nezhad K (2020) Study on the gear performance of polymer-clay nanocomposites by applying step and constant loading schemes and image analysis. Wear 458:203412
54. Rajakumar PR, Nanthini R (2011) Thermal and morphological behaviours of polybutylene terephthalate/polyethylene terephthalate blend nanocomposites. Rasayan J Chem 4(3):567–579
55. Schampera B, Solc R, Woche SK, Mikutta R, Dultz S, Guggenberger G, Tunega D (2015) Surface structure of organoclays as examined by X-ray photoelectron spectroscopy and molecular dynamics simulations. Clay Miner 50(3):353–367
56. Moore DM, Reynolds RC (1997) X-ray diffraction and the identification and analysis of clay analysis of clay minerals. Oxford University Press, Oxford
57. Iulianelli GC, Sebastião PJO, Tavares MIB, dos Santos FA (2015) Influence of organoclay structure on nanostructured materials based on EVA. Mater Sci Appl 6(10):860
58. Akar AÖ, Yıldız ÜH, Tayfun Ü (2023) Halloysite nanotube loaded polyamide nanocomposites: Structural, morphological, mechanical, thermal and processing behaviors. AIP Conf Proc 2607:070005
59. Xia L, Xu Z, Sun L, Caveney PM, Zhang M (2013) Nanofillers to tune Young's modulus of silicone matrix. J Nanopart Res 15:1570
60. Kaplan A, Erdem A, Arslan C, Savas S, Tayfun U, Dogan M (2023) The roles of filler amount and particle geometry on the mechanical, thermal, and tribological performance of polyamide 6 containing silicon-based nano-additives. Silicon 15(7):3165–3180
61. Liu SP, Hwang SS, Yeh JM, Hung CC (2011) Mechanical properties of polyamide-6/montmorillonite nanocomposites-prepared by the twin-screw extruder mixed technique. Int Commun Heat Mass Transfer 38:37–43
62. Mohamed ST, Tirkes S, Akar AO, Tayfun U (2020) Hybrid nanocomposites of elastomeric polyurethane containing halloysite nanotubes and POSS nanoparticles: tensile, hardness, damping and abrasion performance. Clay Miner 55(4):281–292
63. Taheri S, Sadeghi GMM (2015) Microstructure–property relationships of organo-montmorillonite/polyurethane nanocomposites: influence of hard segment content. Appl Clay Sci 114:430–439
64. Shah KJ, Shukla AD, Shah DO, Imae T (2016) Effect of organic modifiers on dispersion of organoclay in polymer nanocomposites to improve mechanical properties. Polymer 97:525–532
65. Alyamac E, Yilmazer U (2004) Dynamics of nanocomposite formation and impact modification of polyethyleneterephthalate. MRS Online Proceedings Library 856:BB7–12
66. Soudmand BH, Shelesh-Nezhad K, Hassanifard S (2020) Toughness evaluation of poly (butylene terephthalate) nanocomposites. Theoret Appl Fract Mech 108:102662
67. Soudmand BH, Shelesh-Nezhad K, Salimi Y (2020) A combined differential scanning calorimetry-dynamic mechanical thermal analysis approach for the estimation of constrained phases in thermoplastic polymer nanocomposites. J Appl Polym Sci 137(41):49260